Accelerated Cataract Formation and Reduced Lens Epithelial Water Permeability in Aquaporin-1-Deficient Mice

Javier Ruiz-Ederra and A. S. Verkman

Purpose. To investigate the involvement of aquaporin (AQP)-1 in lens epithelial cell water permeability and maintenance of lens transparency in experimental models of cataract formation.

Methods. Comparative studies were performed on wild-type versus AQP1-null mice. Osmotic water permeability was measured in calcein-stained epithelial cells in intact lenses from fluorescence changes in response to osmotic gradients. Lens water content was measured by gravimetry using kerosene–bromobenzene density gradients, and from wet/dry weight measurements. Lens transparency was measured by contrast analysis of transmitted grid images. Cataract formation was induced in vitro by incubation in high-glucose solutions and in vivo by acetaminophen toxicity.

Results. Immunofluorescence showed AQP1 expression in wild-type mice in epithelial cells covering the anterior surface of the lens. AQP1 deletion did not alter baseline lens morphology or transparency, though basal water content was ~3% greater ($P < 0.001$). AQP1 deficiency reduced plasma membrane water permeability in lens epithelium by 2.8 ± 0.3-fold ($P < 0.0001$). Loss of lens transparency was accelerated by more than 50-fold in AQP1-null lenses bathed in a 55-mM glucose solution for 18 hours. At 4 hours after acetaminophen administration in 3-methylcholantrene–treated mice, lens opacification was seen in none of the six wild-type mice and in six of six AQP1-null mice.

Conclusions. Lens AQP1 facilitates the maintenance of transparency and opposes cataract formation. (*Invest Ophthalmol Vis Sci.* 2006;47:3960–3967) DOI:10.1167/iovs.06-0229

Cataract is a leading cause of blindness worldwide, with 1.3 million cataract operations performed annually in the United States.[1] Lens opacification is a multifactorial process, in which posttranslational modification of lens structural proteins enhances their aggregation, fragmentation, and precipitation, leading to cataract formation.[2] The lens is an avascular tissue composed of concentric layers of epithelial cells at various stages of differentiation.[3,4] An epithelial cell monolayer extends from the anterior pole of the lens to its equatorial surface, surrounding the elongated lens fibers, which are arranged in a stratified manner with the oldest fibers in the lens interior. Nourishment to the lens is provided by diffusion from the aqueous and vitreous humors. However, it is thought that simple diffusion cannot sustain the metabolic needs of the lens interior.[5] A *circulatory system* has been proposed, in which an asymmetric distribution of ion pumps, transporters, channels, and cell junctions drive ion-coupled fluid absorption, facilitating the entry of nutrients and metabolites into the inner lens across the polar regions and their exit through the lens equator.[6,7]

The aquaporins (AQPs) are a family of water channels that facilitate bidirectional osmotic water transport across cell plasma membranes and, in some cases, the transport of glycerol and other small solutes.[8,9] Phenotype analysis of AQP-null mice has indicated the involvement of AQPs in several aspects of eye physiology, including the maintenance of corneal transparency,[10] corneal wound healing,[11] tear film homeostasis,[12] intraocular pressure regulation,[13] and retinal signal transduction[14] and response to ischemia.[15] Two aquaporins are expressed in the lens, with a polarized distribution: AQP1 in the anterior pole in epithelial cells and AQP0 (also referred to as major intrinsic protein, MIP) in the posterior pole and in nuclear fibers.[16–18] Mutations in AQP0 are associated with hereditary cataracts in mice[19] and humans.[20] Cataracts were not reported in rare humans with AQP1 deficiency,[21] nor have spontaneous cataracts been seen grossly in AQP1-null mice (our unpublished observations). However, in our recent experimental model of intraocular pressure elevation,[22] we observed a delay in the restoration of lens transparency in the AQP1-null mice after mechanical stress induced during the experimental procedure (unpublished observations).

The role of AQP1 in lens epithelium is unknown. We tested the hypothesis that AQP1 is involved in lens water permeability and maintenance of lens transparency. The motivations for this work included (1) the consistent expression of AQP1 in lens epithelium across multiple mammalian species; (2) the involvement of corneal endothelial AQP1 in the maintenance of corneal transparency[10]; and (3) our observations on lens opacification in AQP1-null mice during eye surgery. In this study, we demonstrated for the first time AQP1 expression and water channel function in mouse lens epithelium. Although AQP1 deficiency was not associated with demonstrable abnormalities in baseline lens structure or transparency, we found remarkably accelerated cataractogenesis in both in vitro and in vivo models of cataract formation. Our results provide evidence for a novel role of AQP1 in ocular physiology.

Materials and Methods

Mice

Wild-type and AQP1-deficient mice in a CD1 genetic background matched by age (8–10 weeks) were used, with littermates used in most experiments. Transgenic mice deficient in AQP1 were generated by

From the Departments of Medicine and Physiology, Cardiovascular Research Institute, University of California, San Francisco, California.

Supported by National Eye Institute Grant EY13574; National Institute of Diabetes and Digestive and Kidney Diseases Grants DK35124 and DK72517; National Heart, Lung, and Blood Institute Grants HL59198, HL73856, and EB00415; and Research Development Program Grant R613 from the Cystic Fibrosis Foundation. JR-E was supported by a postdoctoral fellowship from Gobierno Vasco.

Submitted for publication March 2, 2006; revised April 25 and May 16, 2006; accepted July 7, 2006.

Disclosure: **J. Ruiz-Ederra**, None; **A.S. Verkman**, None

The publication costs of this article were defrayed in part by page charge payment. This article must therefore be marked "*advertisement*" in accordance with 18 U.S.C. §1734 solely to indicate this fact.

Corresponding author: A. S. Verkman, 1246 Health Sciences East, University of California, San Francisco, CA 94143-0521; verkman@itsa.ucsf.edu.

Investigative Ophthalmology & Visual Science, September 2006, Vol. 47, No. 9

targeted gene disruption as described.[23] Investigators were blinded to mouse genotype information in all functional studies until completion of experiments. All experimental methods and animal care procedures adhered to the ARVO Statement for the Use of Animals in Ophthalmic and Vision Research, and were approved by the University of California, San Francisco Institutional Animal Care and Use Committee (IACUC).

Lens Isolation

Lenses were isolated from globes by a posterior approach in which the corneal surface was placed on PBS-soaked filter paper. The scleral tissue was partitioned into four quadrants and excess tissue removed by cutting the zonules without touching the lens capsule. Special care was taken to avoid damage to the lens epithelium. For measurement of water permeability, lenses were immobilized on a glass coverslip with cyanoacrylate with the epithelium facing up. For measurement of lens water content, immunoblot, and in vitro opacity analysis, lenses were placed in phosphate-buffered saline (PBS), extraction buffer, and 199 medium (Invitrogen-Gibco, Grand Island, NY), respectively.

Histology and Immunohistochemistry

For examination of baseline lens properties, isolated lenses were transferred to a PBS-containing well with the anterior surface facing up. Digital images were acquired with a stereo-zoom microscope (SMZ1500; Nikon, Tokyo, Japan) equipped with a 1.6× objective lens (working distance, 24 mm; numerical aperture 0.21) and digital camera (Coolsnap HQ; Photometrics, Tucson, AZ). Lens diameter (from eight wild-type and eight AQP1-null mice) was measured using image analysis software (Spot; Universal Imaging, Sterling Heights, MI). For analysis of the epithelial cell morphology, lenses were loaded with calcein and mounted in a custom perfusion chamber, as described later, for water permeability measurements. Fluorescently stained epithelial cells on the lens surface were imaged with an epifluorescence microscope (Leica, Heidelberg, Germany) equipped with a digital camera (Spot; Universal Imaging). For paraffin sections, globes were fixed by immersion in 10% formalin for 48 hours, processed in increasing concentrations of ethanol and then in a clearing agent (Citrisolv; Fisher Scientific, Los Angeles, CA), and embedded in paraffin. Five-micrometer-thick sagittal sections from the central eye were used, taking the optic nerve and pupil as reference points. For immunohistochemistry, sections were deparaffinized in the clearing agent and rehydrated in graded ethanols. After epitope retrieval with citrate buffer (10 mM sodium citrate, 0.05% Tween 20 [pH 6.0], 30 minutes, 95–100°C), sections were blocked with goat serum and incubated with rabbit anti-AQP1 or anti-AQP0 antibodies (both at 1:500; Chemicon, Temecula, CA). Primary antibody was detected with the avidin-biotin complex kit (Vectastain; Vector Laboratories, Burlingame, CA), and developed with 3,3-diaminonzidine. Nuclei were stained with hematoxylin (1:10,000; Fisher Scientific).

Immunoblot Analysis

Lenses of wild-type and AQP1-null mice were isolated and homogenized in 250 mM sucrose, 1 mM EDTA, 2 μg/mL aprotinin, 2 μg/mL pepstatin A, 2 μg/mL leupeptin, and 100 μM serine protease inhibitor (Pefabloc; Sigma-Aldrich, St. Louis, MO). Homogenates were centrifuged at 1500*g* for 10 minutes and the supernatant was loaded onto a 4% to 12% sodium dodecyl sulfate–polyacrylamide gel (10 μg/lane). Protein was transferred to a polyvinylidene difluoride membrane and incubated with rabbit anti-AQP1 or anti-AQP0 antibody (1:1000; Chemicon) or anti-β-actin antibody (1:1000; Sigma-Aldrich), followed by horseradish peroxidase-linked anti-rabbit IgG (1:10,000; GE Healthcare, Piscataway, NJ), and visualized using enhanced chemiluminescence (Roche Diagnostics, Indianapolis, IN). Protein band densitometry was performed (Scion Image for Macintosh; Scion, Frederick, MD), normalizing to actin immunoreactivity.

Calcein-Quenching Measurement of Water Permeability

A calcein-quenching method developed originally for measurement of water permeability in astroglia[24] and used subsequently in corneal cells[12] was adapted for measurement of osmotic water permeability in lens epithelial cells. Cytoplasmic calcein fluorescence is quenched by proteins and is hence sensitive to cell volume. Lenses were loaded with calcein by incubation for 30 minutes with calcein-AM (5 μM; Invitrogen, Eugene, OR) at 37°C. A coverslip with attached lens was mounted in a custom-built perfusion chamber consisting of an acrylic platform containing two perfusion channels and one outlet, in which the coverslip made contact with a small area on the upper surface of the lens (see Fig. 4). The objective lens was focused just outside of the area where the coverslip made contact with the lens. The chamber volume was ~200 μL with a solution exchange half-time of <125 ms at a 40-mL/min perfusion rate. For osmotic water permeability measurements, solutions were exchanged between PBS (300 mOsM) and hypotonic PBS (150 mOsM, 1:1 diluted with water). Solution osmolalities were measured with a freezing-point depression osmometer (Precision Systems, Natick, MA). Calcein fluorescence was measured continuously with an upright epifluorescence microscope (Leitz, Wetzlar, Germany) equipped a 40× air objective (working distance, 0.57 mm; numerical aperture, 0.65), halogen light source (Oriel Instruments, Irvine, CA), 14-dynode photomultiplier, an amplifier, and an analog-to-digital converter. Data were recorded with custom software (written in LabView; National Instruments, Austin, TX). The time course of fluorescence in response osmotic gradients was fitted to a single exponential constant, τ: $F(t) = A + Be^{-t/\tau}$, where A and B are related to system sensitivity and background signal. An approximately linear dependence of calcein fluorescence on cell volume was assumed, as described.[12,24]

Measurement of Lens Water Content

Lens water content was measured by gravimetry (column densitometry), based on a high-precision method developed to measure brain water content.[25] Mixtures of a light solvent (kerosene; K) and a heavy solvent (bromobenzene; BB) were used to prepare a gradient in a 100-mL cylinder. The mixtures consisted of 58.5 mL K+41.5 mL BB adjusted to a specific gravity (sp gr) of 1.1725 (stock A), and 44.36 mL K+55.63 mL BB to give a sp gr of 1.0750 (stock B). These values were determined empirically from pilot studies performed on lenses by using a wide gradient. With the two stocks, 10 mixtures were made (10 mL each) with different proportions (from 10:0 to 2:8 parts of A and B, respectively). The 10 mixtures were carefully layered using PE-60 polyethylene tubing (0.76 mm inner diameter) and the column allowed to stand for 60 to 90 minutes to linearize. Final sp gr was 1.1725 on the bottom and 1.0950 on the top of the column.

Each column was calibrated with solution standards consisting of NaCl (dried in a vacuum oven at 100°C overnight) dissolved in purified water. Four stock solutions were prepared containing 21, 19, 17, and 15 g of NaCl per 100 mL water, corresponding to specific gravities of 1.1579, 1.1418, 1.1260, and 1.1105, respectively Just before lens gravimetry measurements, 3 μL aliquots of each standard were gently placed on top the column with a pipette, and their position in the column recorded after 1 minute. For measurements on lenses, immediately after removal, the left lens of each mouse was incubated for 10 minutes in 300 mOsM PBS, and the right lens in 200 mOsM PBS. Before transferring to the column, excess surface fluid was removed by gentle rolling lenses on an eye spear (Merocel; Medtronic Solan, Jacksonville, FL). Lens sp gr was determined from its position in the column at 2 minutes, using NaCl calibration data to convert position to sp gr.

In some experiments, lens water content was estimated by wet-to-dry weight measurements. Freshly excised lenses (12 from wild-type and 12 from AQP1-null mice) were weighed, dried in a vacuum at 130°C until constant weight was attained (generally 2 days), and weighed. Weight pairs from each lens were used to compute percentage water content.

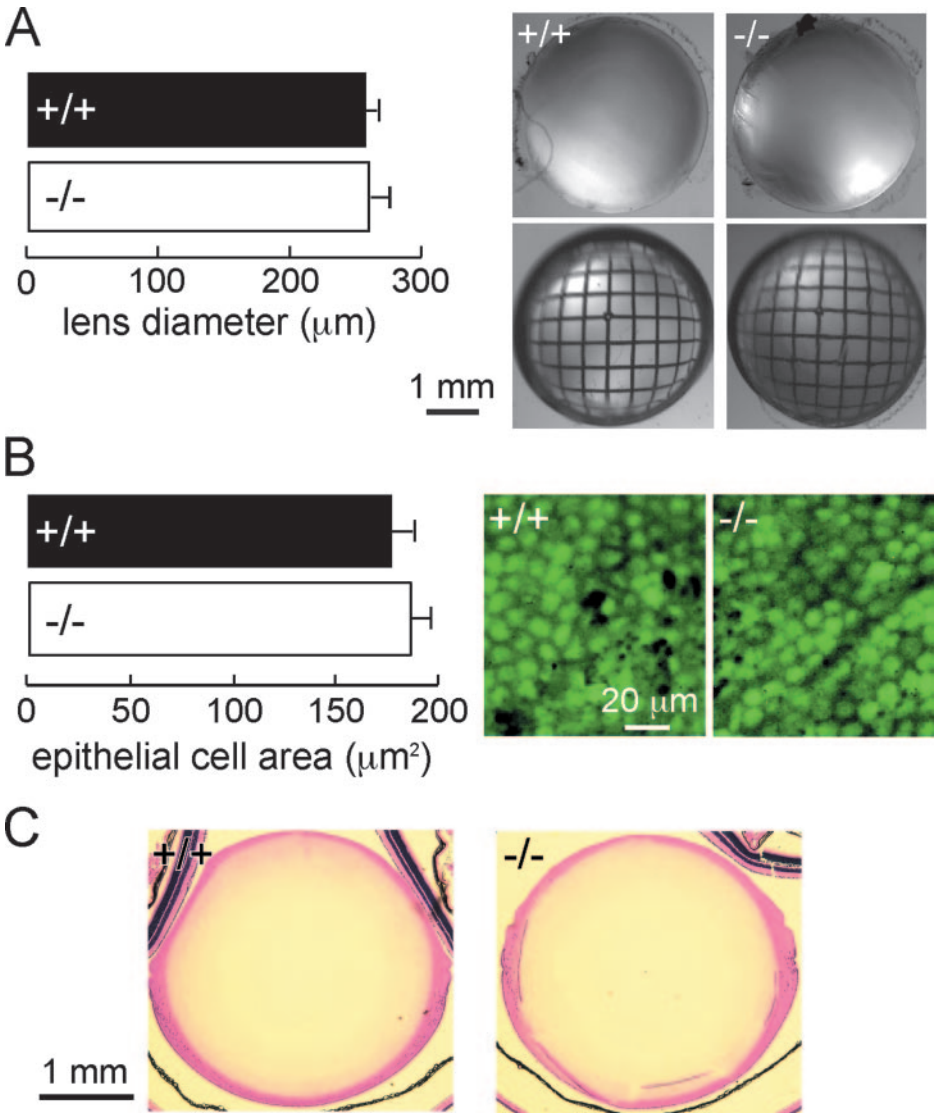

FIGURE 1. Properties of lenses from wild-type and AQP1-null mice. (**A**) *Left:* lens diameter (mean ± SE, six lenses per genotype); *right*: transmitted light photographs of lenses. Lenses on *bottom* panels were placed above grids and focus adjusted to give sharp grid images. (**B**) *Left*: area of epithelial cells at the lens anterior surface (SE, three lenses per genotype); *right*: fluorescence micrographs of lenses after epithelial cell staining with calcein. (**C**) Hematoxylin and eosin–stained paraffin sections of lenses.

In Vitro Model of Cataract Formation

A high-glucose model of in vitro cataractogenesis was used as described.[26,27] Lenses were isolated and transferred to 24-well tissue culture plates containing medium 199 supplemented with 55.6 mM glucose, 25 mM HEPES, 100 U · mL^{-1} penicillin, and 100 mg/mL streptomycin. Incubations were performed at 37°C in a humidified atmosphere containing 5% CO_2 Control lenses were processed identically but with a normal glucose concentration of 5.56 mM. After 18 to 20 hours, lens opacity was quantified with a stereo-zoom microscope (SMZ1500; Nikon) and digital camera (Coolsnap HQ; Photometrics). As diagrammed (Fig. 5A), lenses were placed on a metal grid used for transmission electron microscopy, illuminated from below with monochromatic green light (λ = 515 nm), and imaged after manual focus. Contrast ratios (maximum-to-minimum transmitted signal) were determined from 16 linear scans per image, averaging intensities of grid versus nongrid regions.

In Vivo Model of Cataract Formation

In vivo cataractogenesis was induced by treating mice with the analgesic–antipyretic acetaminophen (Sigma-Aldrich), as described.[28] Mice were pretreated with the cytochrome p-448 inducer, 3-methycholantrene (200 mg/kg in corn oil, 25 mL/kg intraperitoneal). After 48 hours, acetaminophen (700 mg/kg in water, 5 mL/kg IP) was given. Cataract formation was evaluated at 4 hours using a stereozoom microscope (SMZ1500; Nikon). Mice were anesthetized (0.8 L/min oxygen containing 2% isoflurane; Minrad, Bethlehem, PA) and mydriasis was induced 5 minutes before observation with 1 drop of 1% tropicamide. Lens opacification was scored on a 0 to 3 scale (0, no opacity; 3 severe total lens opacification). Some experiments were performed in AQP3-null mice in a CD1 genetic background, generated as described,[29] which manifest polyuria, as do AQP1-null mice. AQP3 is not expressed in the lens.

Statistical Analysis

Data are expressed as the mean ± SE, with statistical comparisons between groups made with the two-tailed Student's *t*-test.

RESULTS

AQP1 Expression in Lens Epithelium and Baseline Lens Properties

Baseline lens morphology and transparency were not altered by AQP1 deletion. Figure 1A (left) shows similar size (diameter) of lenses from wild-type (+/+) and AQP1-null (−/−) mice (P = 0.9). Figure 1A (right) shows photographs of lenses, with the photographs on the bottom showing transmitted light images of grids through the lens. Baseline lens transparency, as quantified by contrast analysis of such transmitted grid images,

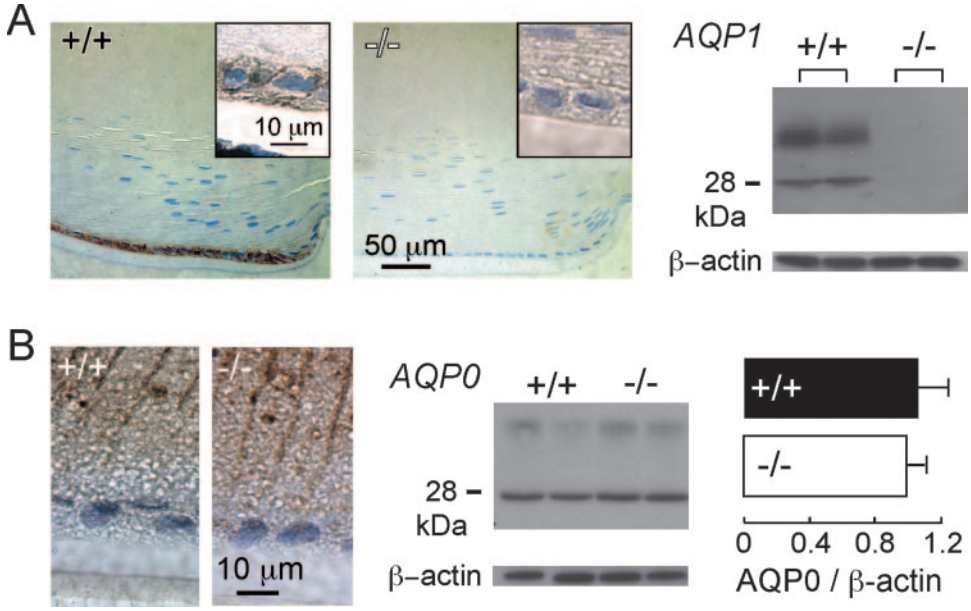

FIGURE 2. Aquaporin expression in mouse lens. (**A**) *Left*: Immunocytochemistry showing AQP1 protein expression (*brown*) in anterior epithelial cells of lens in wild-type mouse; *inset*: high magnification; *middle*: absence of AQP1 immunoreactivity in lens from AQP1-null mouse; *right*: immunoblot analysis of AQP1 in lens homogenates (10 μg protein per lane). (**B**) *Left*: immunocytochemistry showing AQP0 protein expression in lens fiber cells from wild-type and AQP1-deficient lenses. *Middle*: immunoblot analysis of AQP0 (same homogenate as in **A**) and β-actin. *Right*: normalized AQP0/β-actin expression (SE, $n = 4$).

was similar ($P = 0.13$) in wild-type (762 ± 90) and AQP1-null (623 ± 110) mice (see Fig. 5 for details). Lens epithelial cell morphology, assessed after calcein fluorescence staining, was similar in wild-type and AQP1-null mice ($P = 0.23$), as seen grossly or by quantification of epithelial cell area (Fig. 1B). Finally, lens morphology in hematoxylin-eosin–stained paraffin sections showed no differences between phenotypes (Fig. 1C).

Immunocytochemistry showed AQP1 protein expression in epithelial cells at the anterior pole of the lens in wild-type mice, with no specific staining in AQP1-null mice (Fig. 2A). AQP1 staining was seen in both the apical and basolateral membranes of the anterior epithelial cells (Fig. 2A, left; high-magnification inset) and was not detectable in the fiber cells. Immunoblot analysis with AQP1 antibody showed a band at ~28 kDa, corresponding to nonglycosylated AQP1, and a more diffuse band at ~34 kDa, corresponding to glycosylated AQP1 (Fig. 2A, right). These bands were absent in lenses from AQP1-null mice. AQP0 was strongly expressed in lens fiber cells, but was absent in the anterior epithelial cells (Fig. 2B, left). Immunoblot with AQP0 antibody gave a band at ~26 kDa in wild-type and AQP1-null lenses (Fig. 2B, middle). Normalizing for β-actin, AQP1 deletion did not significantly affect lens AQP0 protein expression (Fig. 2B, right).

Lens water content was measured by column densitometry (gravimetry), an approach used extensively for measurement of brain water content. A kerosene/BB density gradient was prepared such that lens density (sp gr) could be determined with great precision (better than 1 part in 1000) from the lens position in the column. NaCl-water standards were used to calibrate the column position with specific gravity (Fig. 3A). Basal water content was significantly greater in lenses from AQP1-null mice ($P < 0.001$), with specific gravities of 1.142 ± 0.001 (wild-type) and 1.132 ± 0.002 (AQP1-null; Fig. 3B), corresponding to a 2.8% ± 0.2% greater basal water content in AQP1-null mice. After a 10-minute incubation in hypotonic saline (200 mOsM), water content in lenses increased, with a significantly greater increase in water content in lenses from wild-type versus AQP1-null mice ($P < 0.05$; Fig. 3C). Basal lens water content was estimated independently from wet and dry lens weights. Using 12 wild-type and 12 AQP1-null lenses, computed percentages of water content were 58.9 ± 0.7 (wild-type) and 61.2 ± 0.9 (AQP1-null). Although there is a trend toward greater water content in AQP1-null lenses, differences did not reach significance ($P = 0.06$). Because of the small size of the mouse lens (weight ~7 mg), wet–dry weight measurements had substantially more variability than column gravimetric measurements.

Reduced Lens Epithelial Water Permeability in AQP1 Deficiency

Osmotic water permeability in lens epithelial cells was measured with a calcein-quenching method from the kinetics of cytoplasmic calcein fluorescence in response to externally applied osmotic gradients (perfusate of 300 vs. 150 mOsM PBS). Measurements were made on calcein-stained lenses in a custom perfusion chamber designed for rapid solution exchange while immobilizing the lens body (Fig. 4A). Cell swell-

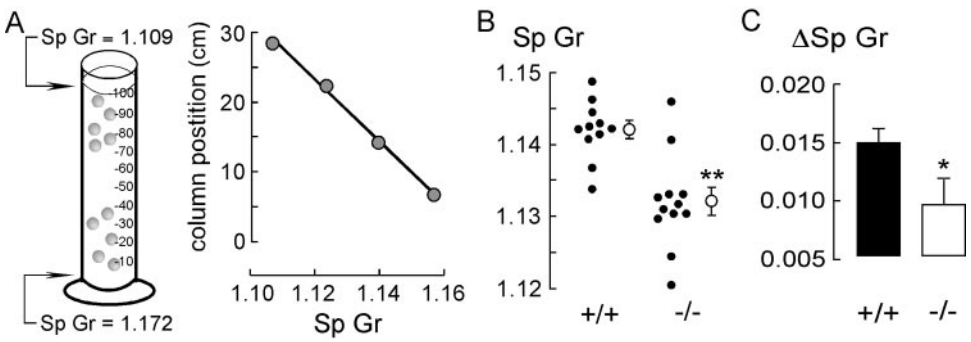

FIGURE 3. Lens water content. (**A**) *Left*: schematic of the BB-kerosene density gradient column used to measure lens water content; *right*: calibration of column position of NaCl/water standards and specific gravity (Sp Gr). Basal water content (**B**) and increase in water content (**C**) after 10 minutes of incubation in hypotonic saline (●, individual lenses; ○ mean ± SE). $^{*}P < 0.05$; $^{**}P < 0.001$.

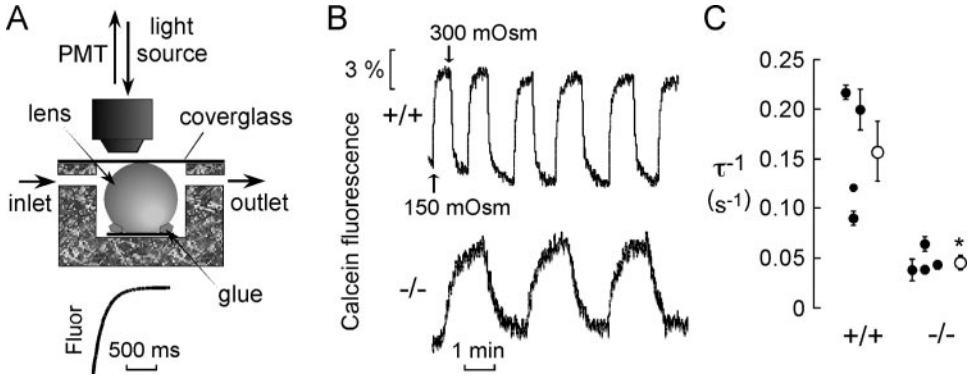

FIGURE 4. Osmotic water permeability in lens epithelial cells. (**A**) *Top*: diagram of lens-perfusion chamber showing freshly isolated lens glued at its posterior pole. The microscope objective was focused just outside of the area where the coverslip made contact with the lens. *Bottom*: chamber solution-exchange time measurement in response to perfusion with PBS followed by dilute fluorescein in PBS. (**B**) Representative calcein fluorescence recordings in response to hypo-osmolar challenge. (**C**) Reciprocal exponential time constants for osmotic equilibration (τ^{-1}, in s^{-1}) in lenses from wild-type and AQP1-null mice. (●) The individual lenses; (○) mean ± SE. $^*P < 0.0001$.

ing dilutes cytoplasmic proteins, resulting in increased cytoplasmic calcein fluorescence (reduced quenching). Lens epithelial cell swelling in response to changing perfusate osmolarity from 300 to 150 mOsM produced a 5% to 8% increase in calcein fluorescence. Figure 4B shows the representative kinetics of reversible cell swelling in response to serial perfusion with solutions of osmolarities of 300 and 150 mOsM. Osmotic equilibration was significantly slowed (3.4 ± 0.6-fold) in lenses from AQP1-null mice ($P < 0.0001$), with τ^{-1} of 0.15 ± 0.03 s^{-1} (wild-type) vs. 0.047 ± 0.006 s^{-1} (AQP1-null; Fig. 4C). Osmotic water permeability coefficients (P_f) of lens epithelial cell membranes, estimated from τ^{-1} and an epithelial cell layer thickness of ~8 μm from histologic sections, were 0.020 cm/s (wild-type) and 0.007 cm/s (AQP1-null). The high P_f in lens epithelial cells in wild-type mice is thus due to AQP1-facilitated osmotic water transport. Our P_f in wild-type mouse lens epithelium is similar to that of 0.012 cm/s measured recently by Varadaraj et al.[30] in freshly isolated rabbit lens epithelial cells.

Accelerated Cataract Formation in AQP1 Deficiency

In vitro and in vivo models were used to investigate the involvement of AQP1 in cataract development. Cataract formation was induced in vitro by incubation of lenses in high glucose–containing solutions at 37°C. Lens opacification was quantified by contrast analysis of transmitted grid images, as shown in Figure 5A. After 18 hours of incubation, all lenses from wild-type mice remained grossly transparent, whereas all lenses from AQP1-null mice showed some degree of opacity. Representative images of four wild-type and four AQP1-deficient lenses are shown in Figure 5B. Some lenses showed focal cortical opacities, representing ~50% of the lens surface, whereas in the more severe cases opacity extended to the entire lens surface. The mean contrast ratio was significantly lower in the lenses from AQP1-null mice, with contrast ratios of 467 ± 20 (wild-type) and 7 ± 2 (AQP1-null; Fig. 5C). From this analysis, lenses from AQP1-null mice showed a 67 ± 5-fold ($P < 0.001$) accelerated loss of transparency.

In vivo cataract formation was studied using an acetaminophen toxicity model in which acetaminophen was administered in 3-methycholantrene pretreated mice. Lenses were examined in anesthetized mice at 4 hours of acetaminophen administration. As shown in Figure 6A, there was little opacification in lenses from wild-type mice, with moderate-to-marked opacification in lenses from AQP1-null mice. Photographs of intact eyes are shown on the left and of freshly enucleated lenses on the right. Opacity scores from a series of

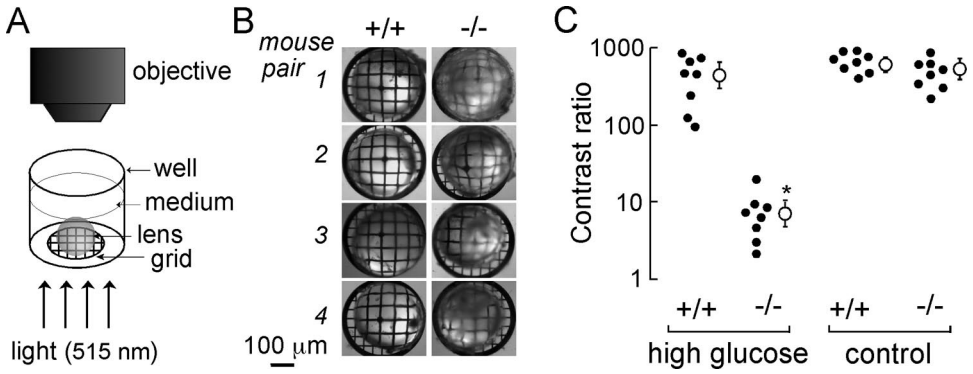

FIGURE 5. In vitro cataract induction by incubation with high-glucose solution. (**A**) Diagram of the apparatus used to quantify lens transparency, showing isolated lens in saline on a metal grid, illuminated from below with monochromatic green light. (**B**) Photographs of grid images transmitted through lenses of four wild-type and four AQP1-deficient mice after an 18-hour incubation in high-glucose solution. (**C**) Contrast ratios of transmitted grid images. Control, measurements on freshly isolated lenses. (●) Individual lenses; (○) mean ± SE. $^*P < 0.0001$.

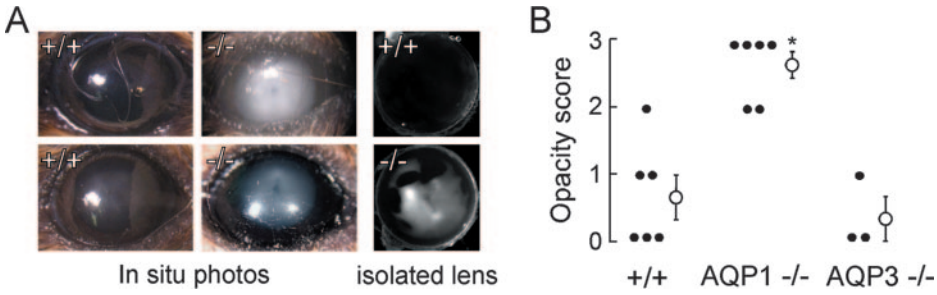

FIGURE 6. In vivo cataract induction by acetaminophen. (**A**) *Left*: representative photographs of eyes of two wild-type and two AQP1-null mice 4 hours after acetaminophen administration. *Right*: Photographs of freshly enucleated lenses. (**B**) Opacification of individual lenses from acetaminophen-treated wild-type, AQP1-null, and AQP3-null mice. Opacity scored from 0 (no opacity) to 3 (severe opacification of entire lens). (●) Individual lenses; (○) mean ± SE. $^*P < 0.001$.

mice, as summarized in Figure 6B, were 2.7 ± 0.3 (wild-type) and 0.7 ± 0.2 (AQP1-null; $P < 0.001$). As a control for possible systemic effects of polyuria in AQP1 null mice, studies were also performed on AQP3-null mice, which are polyuric, similar to AQP1-null mice.[29] The lens opacity score in these identically acetaminophen-treated mice was 0.3 ± 0.3, supporting the data from in vitro studies that the accelerated lens opacification in AQP1-deficient mice is a consequence of lens AQP1 deficiency.

DISCUSSION

We report functional expression of AQP1 in epithelial cells at the anterior pole of mouse lens, and evidence for involvement of AQP1 in maintaining lens transparency in experimental models of cataractogenesis. Lenses of AQP1-null mice did not differ from lenses of wild-type mice in size, gross or histologic appearance, or baseline transparency, yet AQP1-deficient lenses had a small but significantly greater baseline water content than did lenses from wild-type mice. Lenses of AQP1-null mice showed markedly greater opacity than did lenses of wild-type mice in an in vitro model of cataract formation caused by an 18-hour incubation in medium containing high glucose and in an in vivo model of cataract formation caused by acetaminophen toxicity.

The greater water content in AQP1-deficient compared with wild-type lenses was an unexpected observation that may be physiologically relevant to lens fluid movement. Based on the asymmetric distribution of ion pumps, transporters, channels, and cell junctions on the lens surface, a "circulatory" system has been proposed to facilitate nutrient delivery to the lens interior. Current data, albeit indirect, favor circulation of water and solutes around and through the lens, rather than unidirectional flux through the lens.[6] This circulation hypothesis is based on modeling of nonhomogeneous distributions of currents around free-standing rat lenses measured with a vibrating probe.[6,7,31] However, conflicting data have come from studies in isolated rabbit lenses, showing unidirectional fluxes in posterior-to-anterior or anterior-to-posterior directions.[5,32] Recently, measurement of fluid movement in isolated bovine lens using a chamber that separated the lens into three regions (anterior and equatorial epithelial and posterior pole) indicated inward fluid movement at the anterior lens surface, and outward flux at the lens equator and posterior surfaces (Candia et al. *IOVS* 2003;44:ARVO E-Abstract 3455). Although our data do not permit a definitive conclusion about the magnitude or mechanisms of lens fluid movement, they suggest outward fluid flux at the anterior surface and/or the lens equator, because AQP1-null mice manifest reduced anterior surface water permeability and greater basal water content.

Incubation of lenses in high-glucose medium has been used in many studies to test the cataractogenic effects of various metabolites, drugs, and chemicals.[26,28,33] The glucose concentration required in vitro for cataract induction is in accordance with that reported in vivo for permeation of glucose in diabetic cataracts.[34] Current mechanisms proposed to link hyperglycemia and cataractogenesis include nonenzymatic glycation of lens proteins, oxidative stress, and activation of the polyol pathway.[35] Of these mechanisms, the polyol pathway may be related to lens water permeability and water channels, because osmotic homeostasis may be disturbed by conversion of glucose into sorbitol in lenses bathed in high-glucose solutions.[36]

Acetaminophen at high dose has been reported to produce acute anterior cataracts in mice and rabbits.[37,38] In this model cataract formation involves acetaminophen conversion to a toxic reactive semiquinone metabolite (*N*-acetyl-*p*-benzoquinone imine [NAPQI]) by hepatic cytochrome p450. NAPQI is thought to be transported from the liver to the eye through the blood, causing damage to the lens epithelium and anterior cortical cataract.[39] NAPQI is proposed to cause Ca^{2+} release from mitochondria and endoplasmic reticulum of lens epithelial and cortical fiber cells, which may interact with crystalline proteins or activate degradative enzymes, such as calpain, leading to anterior cataract in the cortex, where mitochondria-rich cells are located.[40] In this study, we found evidence of cortical cataract in AQP1-null mice in the acetaminophen toxicity model often at the anterior pole of the lens, where AQP1 is normally expressed.

The mechanisms by which AQP1 protects the lens against opacification in models of cataract formation are uncertain. AQP1 is a water-selective transporting protein, and its deletion in mice produces a variety of abnormalities, including defective urinary concentrating ability,[41] reduced epithelial fluid secretion,[13] and impaired tumor angiogenesis and cell migration.[42] The involvement of AQP1 in each of these processes was ascribable to its water-transporting function (reviewed in Ref. 9). Corneas of AQP1 null mice have reduced baseline thickness, and manifest remarkably greater fluid accumulation and opacification than do wild-type corneas in experimental models of corneal swelling.[10] The mechanisms responsible for impaired maintenance of corneal transparency are unclear, because corneal endothelial cell cultures, although showing reduced osmotic water permeability in AQP1 deficiency, do not show defective isotonic fluid absorption. AQP1 is expressed over the entire surface of the corneal endothelial cell membrane, suggesting high water flux through these membranes.[43] Fischbarg et al.[44] have speculated about the possible involvement of AQP1 in electro-osmotic fluid transport in cornea and in corneal endothelial cell volume regulation, perhaps by interaction of AQP1 with membrane solute transporters.

Similar mechanisms of AQP1-dependent fluid transport could apply in lens, which, like the corneal endothelium, appears to manifest reduced ability to expel excess fluid under stress.

AQP0 is essential for lens transparency.[19,20] It has been estimated that AQP0 constitutes more than 50% of the membrane protein of the lens fibers.[16,17] Unlike AQP1, AQP0 has a widespread distribution throughout lens fibers, but is absent in lens epithelial cells. Another interesting difference is that AQP0 (but not AQP1) water permeability is pH and Ca^{2+} regulated.[45] Also, AQP0 has at least 40 times lower water permeability than does AQP1.[46] Because of its low water permeability it has been proposed that AQP0 may be involved in regulating the resistance of the paracellular pathway, rather than in controlling cell membrane water permeability.[4] Although there is direct evidence against AQP0 function as a gap junction channel,[16] recent studies showed specific microdomain arrangements and interactions of AQP0 with different membrane proteins, suggesting AQP0 involvement in fiber–fiber adhesion.[4] Another proposed role of AQP0 is in acting as a scaffold for organizing γ-crystallins in lens fibers.[47] The mechanism of cataract formation in individuals bearing AQP0 mutations is not clear. It has been proposed that AQP0 facilitates fiber cell adherence, and hence the fiber cell shape, size, and order, that are necessary for lens transparency.[48] AQP0 may also play a role in establishing the refractive index of the crystalline lens, by acting as a conduit for fiber cell dehydration.[20]

Increased water content in the lens nucleus with age is thought to be related to changes in AQP0 content or structure.[49,50] Our results showing increased lens water content in AQP1 deficiency suggest the possibility that reduced lens AQP1 expression with age may be involved as well. Although age-dependent AQP1 expression in mouse lens was not quantified, nor are we aware of such data in human lens, the expression of several AQPs, including AQP1, is reduced with age in nonocular tissues such as kidney.[51]

In conclusion, our study provides the first functional evidence of the role of AQP1 in lens epithelial water permeability, maintenance of normal lens hydration, and protection of the lens from opacification in experimental models of cataractogenesis.

Acknowledgments

The authors thank Liman Qian and Louise Han for mouse breeding and genotype analysis, Eugene Solenov for help in designing the lens perfusion chamber, and Marc H. Levin for helpful advice throughout the investigation.

References

1. Minassian DC, Reidy A, Desai P, Farrow S, Vafidis G, Minassian A. The deficit in cataract surgery in England and Wales and the escalating problem of visual impairment: epidemiological modelling of the population dynamics of cataract. *Br J Ophthalmol*. 2000;84:4–8.
2. Hockwin O, Kojima M, Muller-Breitenkamp U, Wegener A. Lens and cataract research of the 20th century: a review of results, errors and misunderstandings. *Dev Ophthalmol*. 2002;35:1–11.
3. Kuwabara T. The maturation of the lens cell: a morphologic study. *Exp Eye Res*. 1975;20:427–443.
4. Zampighi GA, Eskandari S, Kreman M. Epithelial organization of the mammalian lens. *Exp Eye Res*. 2000;71:415–435.
5. Fischbarg J, Diecke FP, Kuang K, et al. Transport of fluid by lens epithelium. *Am J Physiol*. 1999;276:C548–C557.
6. Mathias RT, Rae JL, Baldo GJ. Physiological properties of the normal lens. *Physiol Rev*. 1997;77:21–50.
7. Candia OA. Electrolyte and fluid transport across corneal, conjunctival and lens epithelia. *Exp Eye Res*. 2004;78:527–535.
8. Agre P, Kozono D. Aquaporin water channels: molecular mechanisms for human diseases. *FEBS Lett*. 2003;555:72–78.
9. Verkman AS. More than just water channels: unexpected cellular roles of aquaporins. *J Cell Sci*. 2005;118:3225–3232.
10. Thiagarajah JR, Verkman AS. Aquaporin deletion in mice reduces corneal water permeability and delays restoration of transparency after swelling. *J Biol Chem*. 2002;277:19139–19144.
11. Levin MH, Verkman AS. Aquaporin-3-dependent cell migration and proliferation during corneal re-epithelialization. *Invest Ophthalmol Vis Sci*. In press.
12. Levin MH, Verkman AS. Aquaporin-dependent water permeation at the mouse ocular surface: in vivo microfluorimetric measurements in cornea and conjunctiva. *Invest Ophthalmol Vis Sci*. 2004;45:4423–4432.
13. Zhang D, Vetrivel L, Verkman AS. Aquaporin deletion in mice reduces intraocular pressure and aqueous fluid production. *J Gen Physiol*. 2002;119:561–569.
14. Li J, Patil RV, Verkman AS. Mildly abnormal retinal function in transgenic mice without Müller cell aquaporin-4 water channels. *Invest Ophthalmol Vis Sci*. 2002;43:573–579.
15. Da T, Verkman AS. Aquaporin-4 gene disruption in mice protects against impaired retinal function and cell death after ischemia. *Invest Ophthalmol Vis Sci*. 2004;45:4477–4483.
16. Bok D, Dockstader J, Horwitz J. Immunocytochemical localization of the lens main intrinsic polypeptide (MIP26) in communicating junctions. *J Cell Biol*. 1982;92:213–220.
17. Fitzgerald PG, Bok D, Horwitz J. Immunocytochemical localization of the main intrinsic polypeptide (MIP) in ultrathin frozen sections of rat lens. *J Cell Biol*. 1983;97:1491–1499.
18. Hasegawa H, Lian SC, Finkbeiner WE, Verkman AS. Extrarenal tissue distribution of CHIP28 water channels by in situ hybridization and antibody staining. *Am J Physiol*. 1994;266:C893–C903.
19. Berry V, Francis P, Kaushal S, Moore A, Bhattacharya S. Missense mutations in MIP underlie autosomal dominant 'polymorphic' and lamellar cataracts linked to 12q. *Nat Genet*. 2000;25:15–17.
20. Shiels A, Bassnett S, Varadaraj K, et al. Optical dysfunction of the crystalline lens in aquaporin-0-deficient mice. *Physiol Genomics*. 2001;7:179–186.
21. Preston GM, Smith BL, Zeidel ML, Moulds JJ, Agre P. Mutations in aquaporin-1 in phenotypically normal humans without functional CHIP water channels. *Science*. 1994;265:1585–1587.
22. Ruiz-Ederra J, Verkman AS. Mouse model of sustained elevation in intraocular pressure produced by episcleral vein occlusion. *Exp Eye Res*. 2006;82:879–884.
23. Ma T, Yang B, Gillespie A, Carlson EJ, Epstein CJ, Verkman AS. Severely impaired urinary concentrating ability in transgenic mice lacking aquaporin-1 water channels. *J Biol Chem*. 1998;273:4296–4299.
24. Solenov E, Watanabe H, Manley GT, Verkman AS. Sevenfold-reduced osmotic water permeability in primary astrocyte cultures from AQP-4-deficient mice, measured by a fluorescence quenching method. *Am J Physiol*. 2004;286:C426–C432.
25. Marmarou A, Poll W, Shulman K, Bhagavan H. A simple gravimetric technique for measurement of cerebral edema. *J Neurosurg*. 1978;49:530–537.
26. Creighton MO, Stewart-DeHaan PJ, Ross WM, Sanwal M, Trevithick JR. Modelling cortical cataractogenesis: 1. In vitro effects of glucose, sorbitol and fructose on intact rat lenses in medium 199. *Can J Ophthalmol*. 1980;15:183–188.
27. Olofsson EM, Marklund SL, Karlsson K, Brannstrom T, Behndig A. In vitro glucose-induced cataract in copper-zinc superoxide dismutase null mice. *Exp Eye Res*. 2005;81:639–646.
28. Lubek BM, Avaria M, Basu PK, Wells PG. Pharmacological studies on the in vivo cataractogenicity of acetaminophen in mice and rabbits. *Fundam Appl Toxicol*. 1988;10:596–606.
29. Ma T, Song Y, Yang B, et al. Nephrogenic diabetes insipidus in mice lacking aquaporin-3 water channels. *Proc Natl Acad Sci USA*. 2000;97:4386–4391.
30. Varadaraj K, Kumari S, Shiels A, Mathias RT. Regulation of aquaporin water permeability in the lens. *Invest Ophthalmol Vis Sci*. 2005;46:1393–1402.
31. Robinson KR, Patterson JW. Localization of steady currents in the lens. *Curr Eye Res*. 1982;12:843–847.
32. Fowlks WL. Demonstration of a net movement of water through the lens. *Experientia*. 1973;29:548–549.

33. Argirova MD, Argirov OK. Region-specific pathophysiological alterations occurring in calf lenses in vitro during hyperglycemia. *Graefes Arch Clin Exp Ophthalmol*. 2002;240:126–130.
34. Kuck J. The formation of fructose in the ocular lens. *Arch Ophthalmol*. 1961;65:840–846.
35. Kyselova Z, Stefek M, Bauer V. Pharmacological prevention of diabetic cataract. *J Diabetes Complications*. 2004;18:129–140.
36. Williamson JR, Chang K, Frangos M, et al. Hyperglycemic pseudohypoxia and diabetic complications. *Diabetes*. 1993;42: 801–813.
37. Shichi H, Gaasterland DE, Jensen NM, Nebert DW. Ah locus: genetic differences in susceptibility to cataracts induced by acetaminophen. *Science*. 1978;200:539–541.
38. Wells PG, Wilson B, Winn LM, Lubek BM. In vivo murine studies on the biochemical mechanism of acetaminophen cataractogenicity. *Can J Physiol Pharmacol*. 1995;73:1123–1129.
39. Zhao C, Shichi H. Histocytological study on the possible mechanism of acetaminophen cataractogenesis in mouse eye. *Exp Mol Pathol*. 1995;63:118–128.
40. Qian W, Shichi H. Cataract formation by a semiquinone metabolite of acetaminophen in mice: possible involvement of Ca^{2+} and calpain activation. *Exp Eye Res*. 2000;71:567–574.
41. Schnermann J, Chou CL, Ma T, Traynor T, Knepper MA, Verkman AS. Defective proximal tubular fluid reabsorption in transgenic aquaporin-1 null mice. *Proc Natl Acad Sci USA*. 1998;95:9660–9664.
42. Saadoun S, Papadopoulos MC, Hara-Chikuma M, Verkman AS. Impairment of angiogenesis and cell migration by targeted aquaporin-1 gene disruption. *Nature*. 2005;434:786–792.
43. Li J, Kuang K, Nielsen S, Fischbarg J. Molecular identification and immunolocalization of the water channel protein aquaporin 1 in CBCECs. *Invest Ophthalmol Vis Sci*. 1999;40:1288–1292.
44. Sanchez JM, Li Y, Rubashkin A, et al. Evidence for a central role for electro-osmosis in fluid transport by corneal endothelium. *J Membr Biol*. 2002;187:37–50.
45. Nemeth-Cahalan KL, Hall JE. pH and calcium regulate the water permeability of aquaporin 0. *J Biol Chem*. 2000;275:6777–6782.
46. Yang B, Verkman AS. Water and glycerol permeabilities of aquaporins 1–5 and MIP determined quantitatively by expression of epitope-tagged constructs in Xenopus oocytes. *J Biol Chem*. 1997; 272:16140–16146.
47. Fan J, Donovan AK, Ledee DR, Zelenka PS, Fariss RN, Chepelinsky γE. γE-crystallin recruitment to the plasma membrane by specific interaction between lens MIP/aquaporin-0 and γE-crystallin. *Invest Ophthalmol Vis Sci*. 2004;45:863–871.
48. Fotiadis D, Hasler L, Muller DJ, Stahlberg H, Kistler J, Engel A. Surface tongue-and-groove contours on lens MIP facilitate cell-to-cell adherence. *J Mol Biol*. 2000;300:779–789.
49. Siebinga I, Vrensen GF, De Mul FF, Greve J. Age-related changes in local water and protein content of human eye lenses measured by Raman microspectroscopy. *Exp Eye Res*. 1991;53:233–239.
50. Lee MD, King LS, Agre P. The aquaporin family of water channel proteins in clinical medicine. *Medicine* (*Baltimore*). 1997;76:141–156.
51. Preisser L, Teillet L, Aliotti S, et al. Downregulation of aquaporin-2 and -3 in aging kidney is independent of V2 vasopressin receptor. *Am J Physiol*. 2000;279:F144–F152.